

# 8×8 MIMO ANTENNA SYSTEM WITH COUPLED-FED ELEMENTS FOR 5G HANDSETS

*Naser Ojaroudi Parchin<sup>1\*</sup>, Yasir Al-Yasir<sup>1</sup>, Ali Alabdullah<sup>1</sup>, Haleh Jahanbakhsh Basherlou<sup>2</sup>, Ahmed Abdulkhaleq<sup>1,3</sup>, Raed A. Abd-Alhameed<sup>1</sup> and James M. Noras<sup>1</sup>*

<sup>1</sup>Faculty of Engineering and Informatics, University of Bradford, Bradford BD7 1DP, UK

<sup>2</sup>Bradford College, Bradford, West Yorkshire, BD7 1AY, UK

<sup>3</sup>SARAS Technology Limited, Leeds LS12 4NQ, UK

\*N.OjaroudiParchin@bradfod.ac.uk

**Keywords:** 5G, DUAL-POLARIZED ANTENNA, LOOP ANTENNA, MIMO, SMARTPHONE ANTENNA

## Abstract

In this paper, a new design of multiple-input/multiple-output (MIMO) antenna is proposed for 3.6 GHz fifth generation (5G) mobile communications. The proposed design contains four pairs of compact microstrip-fed dual-polarized antennas that are symmetrically placed at the four corners of the smartphone printed circuit board (PCB). Each antenna pair consists of a square loop radiation patch and a square defected ground structure (DGS). The loop radiators are fed by two independently coupled T-shaped microstrip feeding lines, which can exhibit radiation pattern and polarization diversity. Therefore, the proposed 5G smartphone antenna design contains four horizontally polarized and four vertically-polarized antennas in total. A low-cost FR-4 dielectric ( $\epsilon=4.4$ ,  $\delta=0.02$ ) with a dimension of  $75 \times 150 \text{ mm}^2$  is used as the PCB substrate. The characteristics of the smartphone antenna are examined using both simulations and measurements. It offers good isolation, dual-polarized full radiation coverage, and sufficient efficiency. In addition, the calculated envelope correlation coefficient (ECC) and total active reflection coefficient (TARC) of the design are very low over the entire operation band.

## 1 Introduction

MIMO systems, which have multiple-antenna units at both transmitter and receiver sides, can take advantage of the multipath components sufficiently to enhance the performance of wireless systems [1]. As MIMO technology can significantly enhance the capacity of the system and resist multipath fading, it has become a hot spot in the field of wireless communication [2-4]. MIMO system has been employed in fourth-generation (4G) handheld devices and it is a promising technology to be used in the future 5G user equipment [5,6]. To realize the MIMO operation for 5G smartphones, the multi-antenna design can be used for having polarization and pattern diversity for reliable communication with minimum mutual coupling [7,8].

According to the requirement of cellular communications, wideband, compact, and high isolation antennas is an urgent demand in the future mobile terminal and the portable applications [9-11]. Among various MIMO antennas, printed antennas are more appropriate due to their low profile, low cost, easy integration, and manufacturability [12]. Recently, several MIMO antenna designs are reported for smartphones at sub-6-GHz operation band [13-17]. However, these smartphone antennas either exhibit narrow impedance-bandwidth, use single-fed/single-polarized radiators, or employ uniplanar structures occupying large spaces of the PCB lead to increase the system complexity.

We propose here a new design of four-element/eight-port 5G smartphone MIMO antenna providing wide impedance bandwidth and polarization/pattern diversity function. The designed 5G antenna is operating at 3.6 GHz, a candidate

frequency band for sub-6-GHz 5G cellular networks [18]. The configuration of the designed antenna array comprises four pairs of dual-polarized loop antenna radiators placed at different corners of the smartphone PCB. In order to improve the port isolation and reduce the mutual coupling, the loop radiation patch is fed by coupled T-shaped microstrip feed-lines. By exciting the radiator from the coupled feed lines, two orthogonally polarized waves are generated. The design not only generates dual-polarizations but also provides the required full radiation coverage. The proposed 5G smartphone antenna array was properly fabricated on an FR-4 substrate and tested in the Antenna Laboratory of Bradford University, UK. Good impedance and isolation over the operation band are achieved. In addition, sufficient MIMO performance in terms of ECC and TARC characteristics has been obtained. Furthermore, the antenna  $S_{nn}$  results in the presence of smartphone components is investigated. The fundamental properties of the single-element antenna and its MIMO design are elaborated below.

## 2. Single-Element Antenna

In this section, the fundamental characteristics of the single-element antenna have been discussed. Figure 1 depicts the schematic of the designed dual-polarized antenna. As illustrated, it is composed of a square loop radiator with a pair of coupled T-shaped microstrip feeding lines. In addition, a square slot is inserted in the back layer of the substrate to improve the antenna radiation performance. The parameter values of the designs (single-element and the MIMO smartphone antennas) are listed in Table 1.

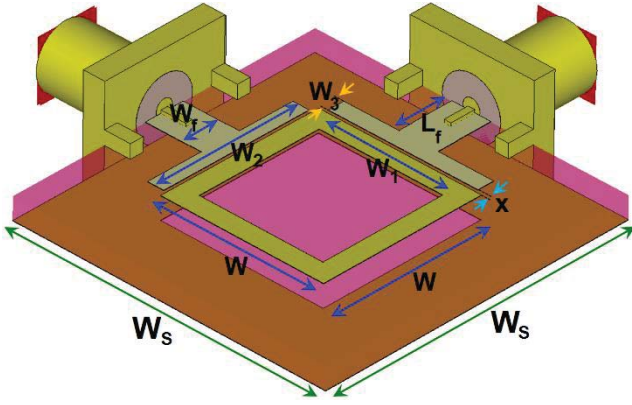


Fig. 1. Schematic of the single-element/dual-polarized antenna design.

Table 1 Parameter values of the proposed antenna design.

Parameter	$W_s$	$W_{sub}$	$L_{sub}$	$h_{sub}$	$W$
Value (mm)	24	75	150	1.6	12.5
Parameter	$W_1$	$W_2$	$W_3$	$W_f$	$L_f$
Value (mm)	9.5	11.5	1.9	3	0.2

Different structures and S parameters of the dual-polarized antenna with a square patch radiator (Ant. a), with a square loop radiator (Ant. b), and the proposed design (Ant. c) are shown and compared in Fig. 2. As seen, the main resonance of the antenna with a square radiation patch occurs at 5.1 GHz, while by converting it to a square loop, the length of resonator increased and the antenna resonates around 4 GHz. Finally, by cutting a square slot in the ground plane, the antenna can exhibit good impedance-matching function with improved-bandwidth and high isolation characteristics at the desired operation band (3.4-3.8 GHz).

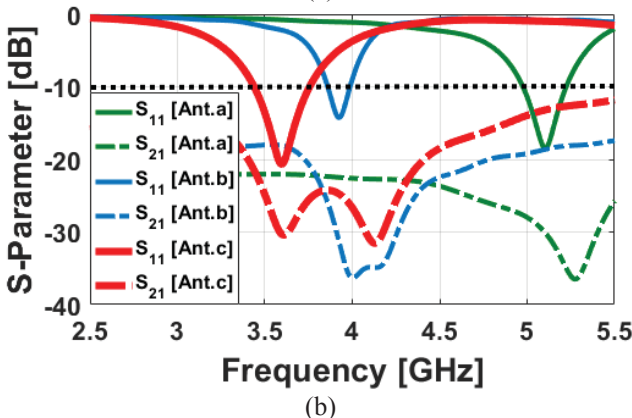
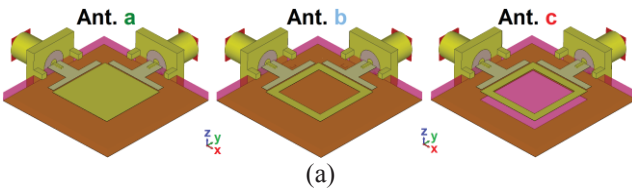


Fig. 2. (a) Various structures and (b) S parameters of the antenna.

Radiation patterns ( $\Phi$ ) of the antenna for different polarizations are illustrated in Figs. 3 (a) and (b). It can be observed that the antenna provides good dual-polarization

characteristics with  $90^\circ$  difference and similar radiation pattern performances with 3.15 dB IEEE gain. Figure 3 (c) shows the fundamental radiation characteristics of the antenna including radiation efficiency (R.E.), total efficiency (T.E.) and maximum gain (M.G.). As shown, the antenna provides more than 70% efficiencies over the frequency range of 3.4 to 3.8 GHz. In addition, more than 3 dBi maximum gain has been achieved for the proposed antenna.

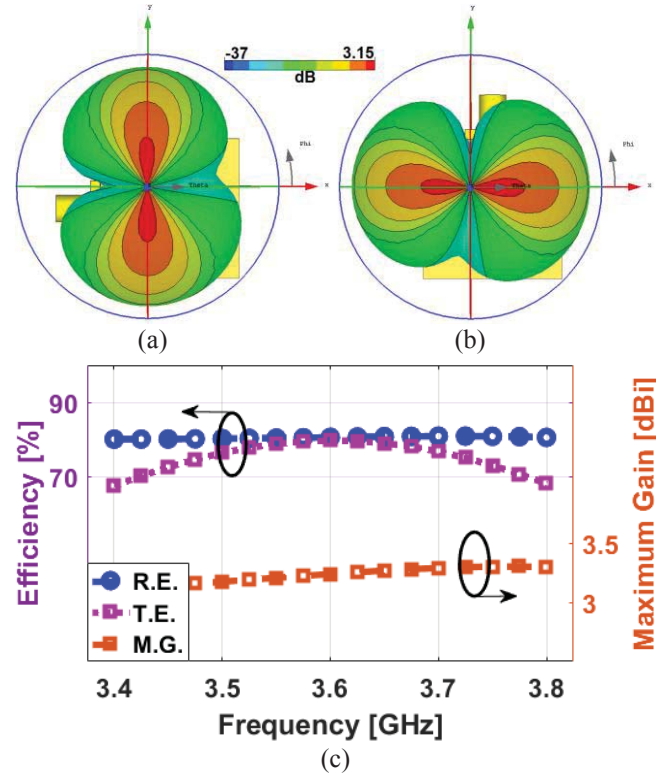


Fig. 3. Radiation patterns ( $\Phi$ ) of the antenna for different polarizations, (a) first port (b), second port, and (c) the fundamental radiation characteristic of the antenna versus its operation band.

### 3. The proposed MIMO antenna system for 5G smartphones

Figure 4 illustrates the configuration of the designed MIMO smartphone antenna. As shown, it comprises of four pairs of dual-polarized loop radiators placed at different corners of the mainboard.

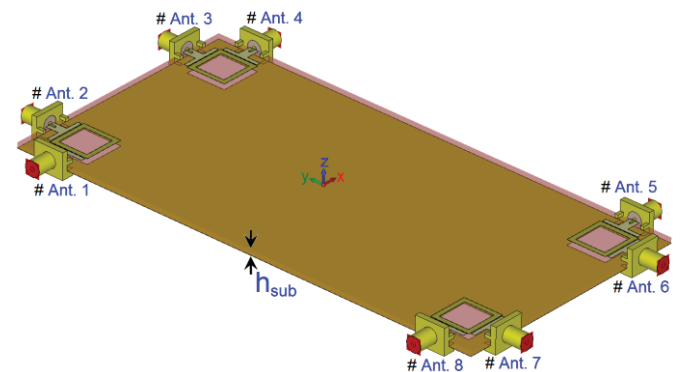


Fig. 4. The proposed MIMO smartphone antenna.

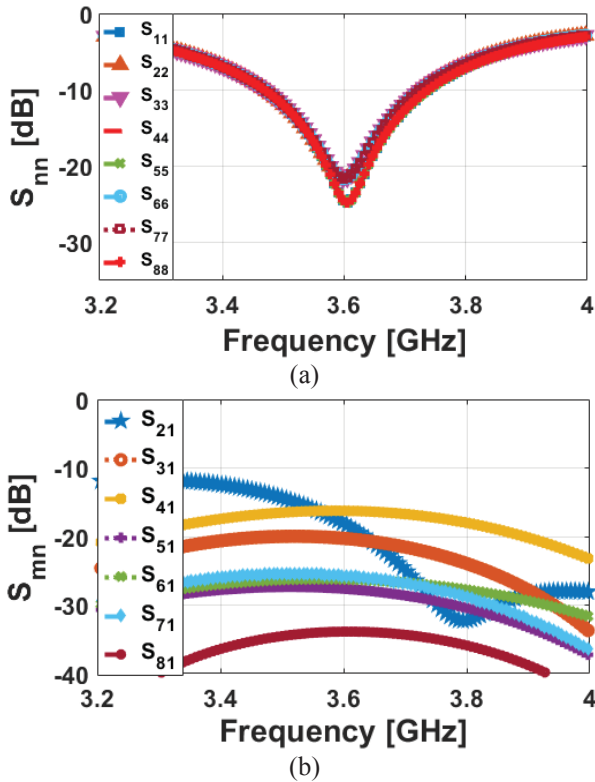


Fig. 5. Simulated (a)  $S_{nn}$  and (b)  $S_{mn}$  of the MIMO design.

Figure 5 depicts the S parameters (including  $S_{nn}$  and  $S_{mn}$ ) of the designed smartphone antenna. As shown, the antenna exhibits good S parameters with more than 300 MHz bandwidth and acceptable isolations of better than 16 dB. Employing the square slots not only improves the impedance-matching and bandwidth of the radiators but also improve the radiation coverage of the main design to cover the top/bottom regions of the main board. Figure 6 depicts the current distributions of Ant. 1 & Ant. 2 at the resonance frequency of 3.6 GHz in the top and bottom layers of the antenna for different feeding ports. It can be observed that the currents are mainly distributed around the loop radiator. In addition, the inserted square slot in the ground plane appears very active with high current densities. Furthermore, as seen, the currents flow contrary to each other for different feeding ports.

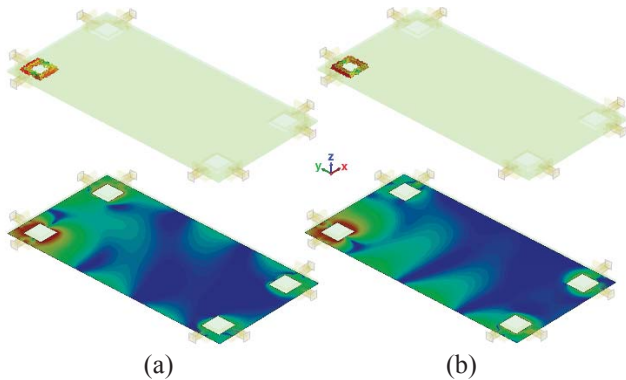


Fig. 6. The current distributions at 3.6 GHz for (a) Ant. 1 and (b) Ant. 2.

Figure 7 shows the side views of the radiation patterns for a single-element radiator (Ant. 1) with and without the interest

square slot. As shown in Fig. 7 (a), the radiation pattern of the antenna without the slot mainly covers the top region of the PCB. Clearly, by inserting the square-slot (Fig. 7 (b)), the antenna elements can provide quasi-symmetrical radiation patterns and improve the radiation coverage of the system [19].

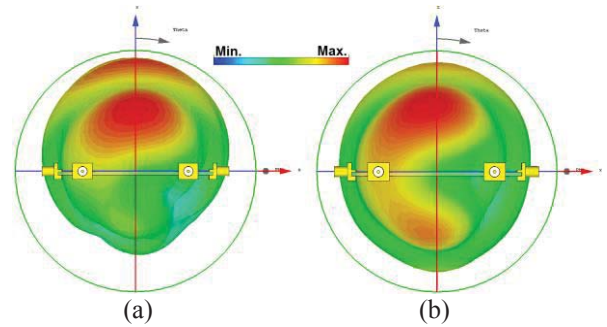


Fig. 7. The radiation pattern of Ant. 1, (a) without and (b) with the inserted DGS.

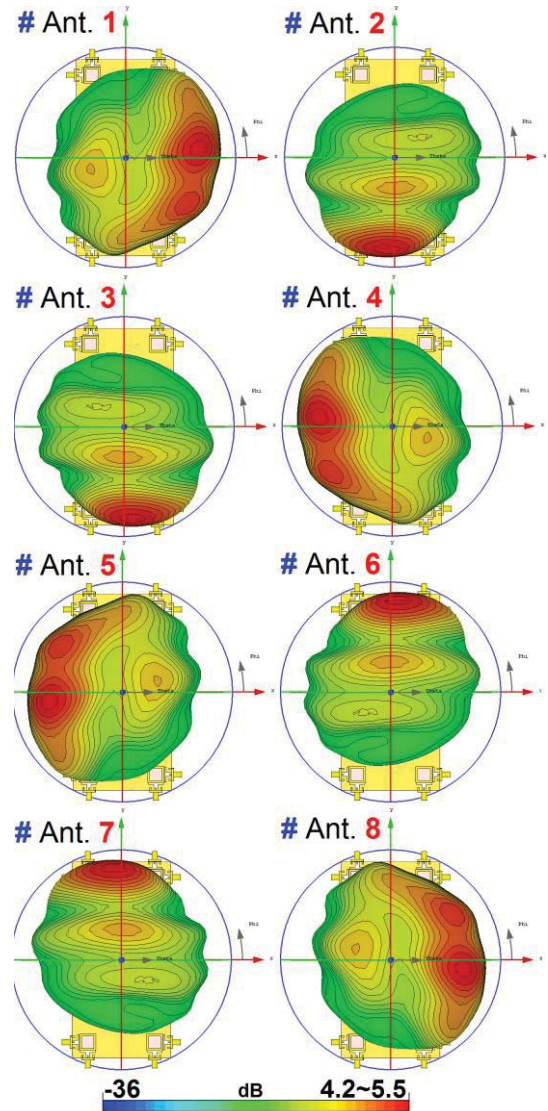


Fig. 8. Radiation patterns of the antenna elements at 3.6 GHz.

The design radiation patterns are displayed in Fig. 8. The 8-element MIMO antenna provides differently polarized radiation patterns for each region of pattern coverage. In other

words, the proposed antenna not only can cover the required radiation pattern coverage but also it provides different polarizations (horizontal/vertical) for each region of the PCB [20]. Furthermore, the antenna provides sufficient radiation and total efficiencies over the operation band, as illustrated in Fig. 9: more than 65% radiation and total efficiencies have been obtained for the radiation elements at 3.6 GHz.

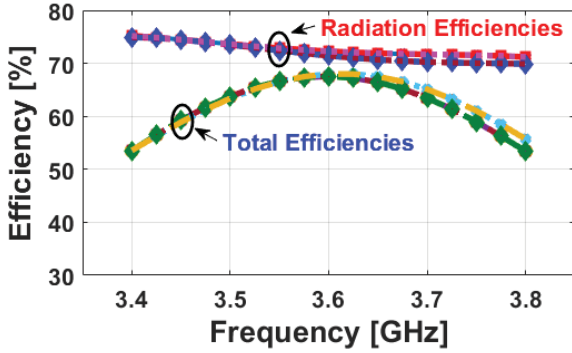


Fig. 9. Radiation and total efficiencies of the design.

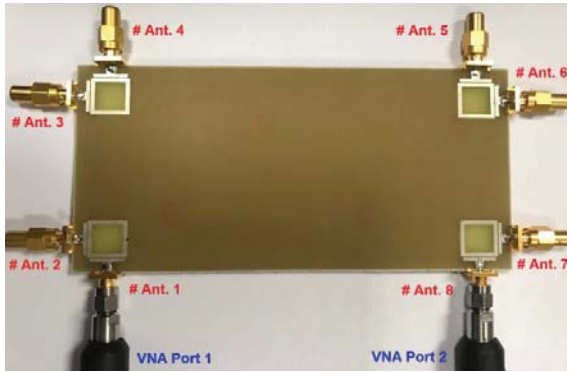


Fig. 10. Fabricated prototype of the smartphone antenna.

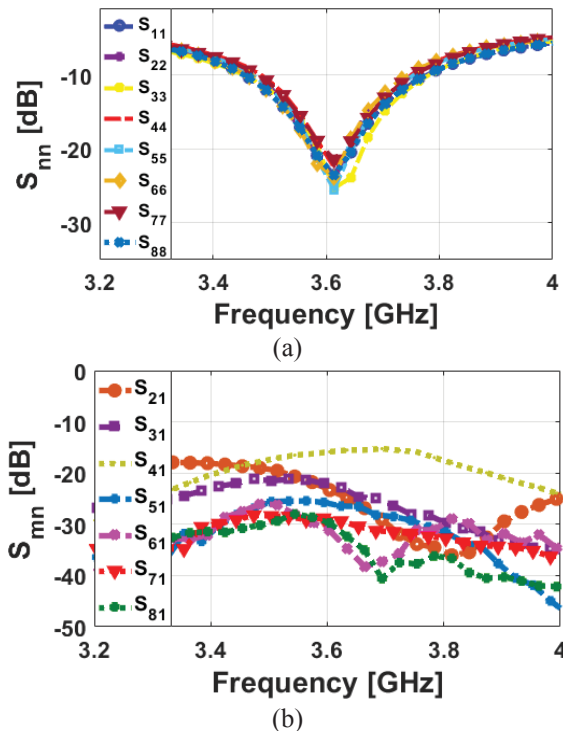


Fig. 11. Measured (a)  $S_{nn}$  and (b)  $S_{mn}$  of the MIMO design.

Figure 10 shows a photograph of the fabricated prototype. The smartphone antenna is constructed on a cheap FR4 substrate with an overall dimension of  $75 \times 150 \times 1.6$  mm<sup>3</sup>. Its fundamental characteristics in terms of S-parameters, radiation patterns, and gain levels are measured. Figures 11 (a) and (b) illustrates the measured  $S_{nn}$  and  $S_{mn}$  results of the fabricated MIMO design: similar  $S_{nn}$  results with wide bandwidth and less than -16 dB  $S_{mn}$  have been achieved for the prototype. Compared with the simulations (shown in Fig. 5), a good agreement is achieved.

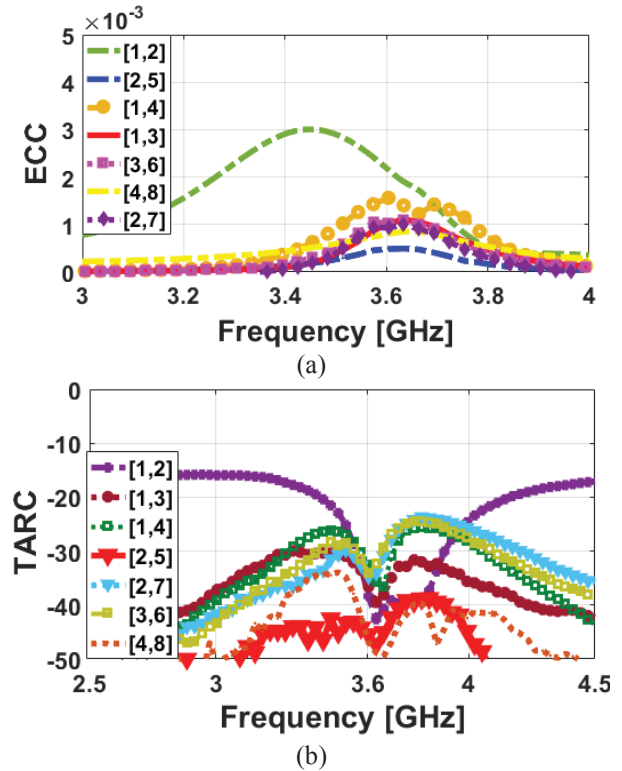


Fig. 12. Calculated (a) ECC and (b) TARC results from measurements.

In order to ensure that the MIMO antenna can work properly, ECC and TARC characteristics are two important parameters to be investigated [21,22]. The ECC and TARC characteristics of MIMO antenna can be calculated from the S-parameters using the formula described as:

$$ECC = \frac{|S_{mm}^* S_{mn} + S_{nm}^* S_{nn}|^2}{(1 - |S_{mm}|^2 - |S_{mn}|^2)(1 - |S_{nm}|^2 - |S_{nn}|^2)^*} \quad (1)$$

$$TARC = -\sqrt{\frac{(S_{mm} + S_{mn})^2 + (S_{nm} + S_{nn})^2}{2}} \quad (2)$$

The calculated ECC and TARC characteristics of the 5G smartphone antenna from measurements are represented in Fig. 12. The calculated ECC results are very low entire the operation bands (less than 0.003). It can be also observed that the TARC value of the design is less than -30 dB at 3.6 GHz. The  $S_{nn}$  ( $S_{11}$ – $S_{88}$ ) characteristic of the proposed smartphone antenna in the presence of battery, speaker, camera, USB connector, and LCD screen are investigated and illustrated in Fig. 13. It can be observed that the antenna provides sufficient  $S_{nn}$  covering 3.6 GHz band with a slight variation.

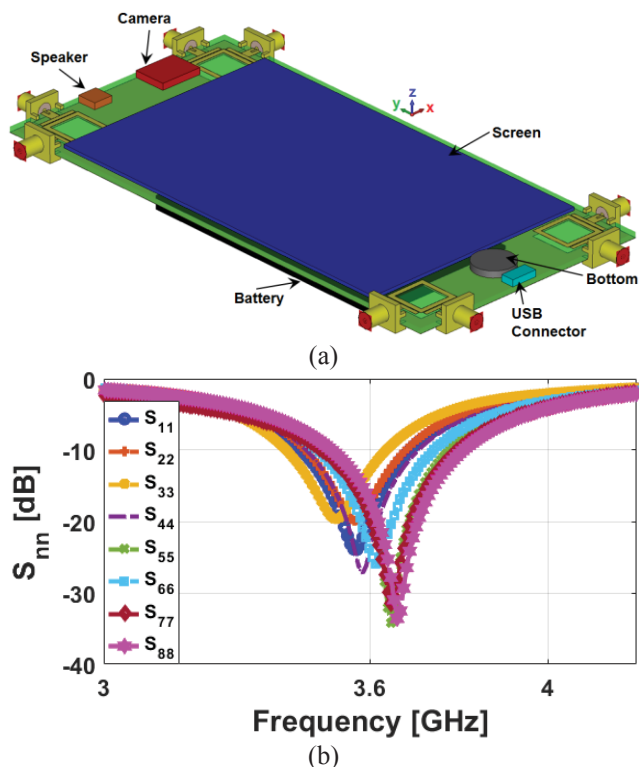


Fig. 13. (a) Schematic and (b)  $S_{nn}$  characteristic of the MIMO antenna in the presence of the smartphone components.

## 4 Conclusion

A design of eight-port smartphone antenna array is proposed for 3.6 GHz cellular communications. Its configuration is composed of four dual-polarized loop antenna elements placed at different corners of the smartphone mainboard with an FR-4 dielectric. In addition, a square DGS has been inserted under each antenna pairs. Acceptable fundamental properties in terms of input-impedance, antenna gain, efficiency, and radiation patterns are achieved.

## 5 Acknowledgments

This project has received funding from the European Union's Horizon 2020 research and innovation program under grant agreement H2020-MSCA-ITN-2016 SECRET-722424.

## 6 References

[1] Jensen, M., Wallace, J.: 'A review of antennas and propagation for MIMO wireless communications', *IEEE Trans. Antennas Propag.*, 2004, 52, 2810–2824

[2] Hassan, N., Fernando, X.: 'Massive MIMO Wireless Networks: An Overview', *Electronics*, 2017, 6, 1-30

[3] Parchin, N. O. et al.: 'Dual-polarized MIMO antenna array design using miniaturized self-complementary structures for 5G smartphone applications', 13th European Conference on Antennas and Propagation (EuCAP), Krakow, Poland, 2019

[4] Ojaroudi, N., Ojaroudi, M.: 'A novel design of triple-band monopole antenna for multi-input multi-output communication', *Microwave and Optical Technology Letters*, 2013, 55, 1258–1262

[5] Kammoun, A. et al.: 'Design of 5G full dimension massive MIMO systems', *IEEE Trans. Commun.*, 2018, 66, 726–740

[6] Hussain, R., Alreshaid, A. T., Podilchak, S. K., Sharawi, M. S.: 'Compact 4G MIMO antenna integrated with a 5G array for current and future mobile handsets', *IET Microw. Antennas Propag.*, 2017, 11, (2), 271-279

[7] Parchin, N. O. et al.: 'Eight-element dual-polarized MIMO slot antenna system for 5G smartphone applications', *IEEE Access*, 2019, 9, 15612–15622

[8] Parchin, N. O. et al.: 'Mobile-phone antenna array with diamond-ring slot elements for 5G massive MIMO systems', *Electronics*, 2019, 8, 521

[9] Parchin, N. O. et al.: 'Recent developments of reconfigurable antennas for current and future wireless communication systems', *Electronics*, 2019, 8, 128

[10] Ojaroudi, N., Ojaroudi, M.: 'Dual-band coplanar waveguide-fed monopole antenna for 2.4/5.8 GHz radiofrequency identification applications', *Microwave and Optical Technology Letters*, 2012, 10, 2426-2429

[11] Parchin, N. O., et al.: 'UWB mm-wave antenna array with quasi omnidirectional beams for 5G handheld devices', *IEEE International Conference on Ubiquitous Wireless Broadband (ICUWB)*, Nanjing, China, 2016, 5–8

[12] Sharawi, M. S.: 'Printed MIMO antenna engineering', (Artech House, 2014)

[13] Li, Y., Luo, Y., Yang, G.: 'High-isolation 3.5-GHz 8-antenna MIMO array using balanced open slot antenna element for 5G smartphones', *IEEE Trans. Antennas Propag.*, 2019, 67, (6), 3820 - 3830

[14] Al-Hadi, A., Ilvonen, J., Valkonen, R., Viikan, V.: 'eight-element antenna array for diversity and MIMO mobile terminal in LTE 3500MHz band', *Microwave Opt. Technol. Lett.*, 2014, 56, 1323- 1327

[15] Sun, L., Feng, H., Li, Y., Zhang, Z.: 'Compact 5G MIMO mobile phone antennas with tightly arranged orthogonal-mode pairs', *IEEE Trans. Antennas Propag.*, 2018, 66, 6364–6369

[16] Abdullah, M.: 'Compact 4-port MIMO antenna system for 5G mobile terminal', In *Proceedings of the International Applied Computational Electromagnetics Society Symposium*, Florence, Italy, March 2017

[17] Zhao, A., Ren, Z.: 'Size reduction of self-isolated MIMO antenna system for 5G mobile phone applications', *IEEE Antennas Wirel. Propag. Lett.*, 2019, 18, 152–156

[18] Statement: Improving Consumer Access to Mobile Services at 3.6 GHz to 3.8 GHz. Available online: <https://www.ofcom.org.uk/consultations-and-statements/category-1/future-use-at-3.6-3.8-ghz> (accessed on 21 October 2018).

[19] Ojaroudi, N., Ghadimi, N.: 'Band-notched UWB slot antenna', *Microwave and Optical Technology Letters*, 2014, 56, 1744-1747

[20] Parchin, N. O. et al.: 'Multi-band MIMO antenna design with user-impact investigation for 4G and 5G mobile terminals', *Sensors*, 2019, 19, 456

[21] Li, M.-Y. et al.: 'Tri-polarized 12-antenna MIMO array for future 5G smartphone applications', *IEEE Access*, 2018, 6, 6160–6170

[22] Sharawi, M. S.: 'Printed multi-band MIMO antenna systems and their performance metrics [wireless corner]', *IEEE Antennas Propag. Mag.*, 2013, 55, 218–232